PHILOSOPHICAL TRANSACTIONS OF THE ROYAL SOCIETY A MATHEMATICAL, PHYSICAL & ENGINEERING SCIENCES

Radioactive nuclear beam facilities based on projectile fragmentation

David J. Morrissey and Bradley M. Sherrill

Phil. Trans. R. Soc. Lond. A 1998 **356**, 1985-2006
doi: 10.1098/rsta.1998.0260

THE ROYAL SOCIETY

Radioactive nuclear beam facilities based on projectile fragmentation

By David J. Morrissey and Bradley M. Sherrill

National Superconducting Cyclotron Laboratory, East Lansing, MI 48824, USA

The production of radioactive ions by using direct in-flight separation techniques is discussed. The reaction mechanisms used to produce radioactive beams near projectile velocities can be broadly divided into four classes: projectile fragmentation, nucleon transfer, fission, and Coulomb excitation. Radioactive nuclei produced by these reactions have large forward momenta with relatively sharp angular distributions peaked close to zero degrees. Such narrow distributions are suitable for collection with magnetic devices. Further beam purification can be achieved by exploiting atomic energy-loss processes in profiled energy degraders combined with a second magnetic selection. Secondary beam intensities of up to 1%, or so, of the primary beam intensity are possible, although the beam emittance depends on the production mechanism and may be poor. The features of the production reaction mechanisms, separation techniques, and a review of worldwide efforts are presented. Also the relative advantages and disadvantages of the method are discussed along with techniques that can be used to overcome some of the disadvantages.

Keywords: radioactive nuclear beams; projectile fragmentation; in-flight separation; magnetic achromatic devices

1. Introduction

Intense beams of a broad range of very exotic nuclei are now routinely produced and used to induce secondary nuclear reactions in laboratories around the world. The technique that has become standard for making these radioactive nuclear beams (RNBs) takes advantage of the kinematic (forward) focusing that occurs in certain peripheral nuclear reactions that occur with heavy projectiles at relatively high incident energies. The exotic ions are then rapidly separated by in-flight techniques before they decay or are stopped. This technique is usually called the 'projectile fragmentation technique', but more correctly might be referred to as in-flight separation since a variety of reaction mechanisms, besides projectile-fragmentation, have been used to produce the nuclei. We will present a review of the production, separation techniques, beam properties, and examples of secondary reactions of the RNBs available from in-flight separators.

The original process of projectile fragmentation, in which very-high-energy nuclei (kinetic energy per nucleon of the order of m_0c^2) are broken into smaller residue nuclei that retain most of the vector momenta of the beam, was studied in the 1970s with the BEVALAC accelerator at the Lawrence Berkeley Laboratory (LBL). In the mid-1970s a technique was developed at LBL to produce radioactive ^{11}C ions from a primary ^{12}C beam. Up to 1% of the incident beam was converted into ^{11}C ions and separated (Alonso *et al*. 1978; Alonso 1984) for implantation in biomedical

samples. Nuclear physics experiments to produce exotic nuclei and space instrument calibrations by using similar techniques based on magnetic rigidity were pioneered with beamline elements at LBL (Viyogi *et al*. 1979), and then dramatically extended by using degraders in the LISE spectrometer at GANIL (Dufour *et al*. 1986; Anne *et al*. 1987). The technique has been further extended with the A1200 separator at the National Superconducting Cyclotron Laboratory (NSCL) (Sherrill *et al*. 1992), the RIPS separator at RIKEN (Kubo *et al*. 1990), the FRS device at GSI (Geissel 1992*a*), and the upgraded LISE-3 system (Mueller & Anne 1991). Several review articles are available on aspects of the in-flight separation technique (Sherrill 1992; Münzenberg 1992; Geissel *et al*. 1995) and this technique is not limited to high-energy beams. A complete programme using a low-energy radioactive beam made by in-flight separation has been established at Notre Dame University, by using superconducting solenoids to provide in-flight separation of direct-reaction products at low energies (Kolata *et al*. 1989; Becchetti *et al*. 1991).

It is interesting to note that the observation of the anomalous reaction cross-section of ^{11}Li by Tanihata *et al*. (1985) was among the first RNB experiments performed with projectile fragments at LBL. These surprising results lead to one of the most intense theoretical and experimental quests in nuclear physics, i.e. understanding the unusual nature of nuclei near the neutron dripline. These first experiments spurred the whole field of nuclear structure to reconsider nuclei far from stability and then created an increased demand for radioactive beams of the most exotic nuclei with a range of kinetic energies. A new generation of experiments is now underway at laboratories around the world, as is evident by the articles in this volume. We should note that nearly every accelerator facility that provides heavy-ion beams has, or is planning to implement, a facility based on in-flight techniques. Those laboratories that are presently operating devote large fractions of research time to these beams, in some cases up to 80%.

The most important feature of the reaction products is that they are produced with velocities near that of the beam and are not stopped nor generally reaccelerated, although a cooler ring has been used for several important experiments. Depending on the ion and target, production reactions that have this property include projectile fragmentation, simple particle transfer or direct reactions, Coulomb dissociation, and fission (for a limited acceptance). Other mechanisms have been used for in-flight separation techniques, for example, fusion–evaporation reactions at Coulomb barrier energies have been used to make beams, and at slightly higher energies, deeply inelastic processes could produce beams at usable intensities (over some limited acceptance due to the less strong kinematic focusing). Separation techniques, such as those discussed below, are applied to produce beams from these reactions. However, a full discussion of all these possibilities is outside the scope of this work and there is a review of mass separator techniques for near-Coulomb barrier energies by Wollnik (1987).

The beam of exotic nuclei must be separated from the primary beam and from the other reaction products by some combination of magnetic, and perhaps electrostatic, elements acting on the distribution of ions. Almost all of the higher energy facilities use achromatic magnetic devices, where achromatic means that the position and angle of ions at the end of the device (called the focal plane) does not depend on the ion's momentum. Such achromatic magnetic devices are generally most useful for efficient separation at the higher energies because they can collect a large fraction

of all the produced fragments and focus them to a small spot. An early paper by Schmidt *et al*. (1987) outlines the fundamentals of the use of achromatic devices.

Electric fields, although desirable because they can provide velocity (kinetic energy) separation, are generally not used by themselves at the higher energies that are characteristic of fragmentation energies because the attainable fields can not sufficiently bend high rigidity fragments. However, Wien filters are used to improve the purity of RNBs. The upgrade of the LISE separator to LISE3 included a high electric field Wien filter to make a velocity separation of fragments separated by the LISE spectrometer (Mueller & Anne 1991). A similar technique has been used at the NSCL in which the RPMS is used (Nolen & Harwood 1985). The range over which this additional separation is still practical ends around 100 MeV per nucleon. Many devices used at lower beam energies employ electric fields to cancel the velocity dispersion of magnetic dipoles leaving only a dispersion in the mass-to-charge ratio (Nolen & Harwood 1985; Davids & Larson 1989; Tribble *et al*. 1989). A detailed discussion of this technique also has been given by Wollnik (1987). The beams from these devices suffer from some contamination, since the separation technique is only sensitive to the *mass-to-charge* ratio of the ion and not strictly the *mass-to-proton number* ratio of the ion. A solution to this ambiguity is the gas-filled separator technique (Rehm *et al*. 1996), in which a spectrograph is filled with a few millibars of gas. The equilibrium charge state of the ion is proportional to velocity so the final position is just determined by the mass of the ion. So far this technique has not been applied to separate RNBs, but plans are being developed at the Argonne National Laboratory to provide beams from the Canadian Penning Trap by such a technique (W. Henning, personal communication). A distinct advantage of the fast-ion achromatic devices is that the purity of the secondary beams can be improved by passing the ions through profiled energy degraders at an intermediate dispersive point (Schmidt *et al*. 1987; Geissel *et al*. 1989). This can, in most cases, eliminate mass-to-charge ambiguities and provide essentially pure secondary beams for even the heaviest elements.

Solenoid magnetic lenses provide very high solid angle collection of forward-going reaction products. Solenoids have the advantage that they are very good collectors, but suffer from the fact that they provide limited mass-to-charge separation. Further, the field strength of present day superconducting solenoids probably limits such devices to fragment energies below 50 MeV per nucleon. The programme at Notre Dame University uses superconducting magnetic solenoids to collect and separate low-energy radioactive beams from a few direct reactions (Kolata *et al*. 1989; Becchetti *et al*. 1991). Other solenoids have been constructed by a group from the University of Michigan at the NSCL (O'Donnell *et al*. 1994) and by Joubert *et al*. (1991) at GANIL.

One of the largest difficulties of beams produced by projectile fragmentation is that the secondary beam emittance is unavoidably large due to the random recoil momentum of the fragment created by the nuclear reaction. This emittance shrinks with increasing beam velocity. None the less, the resulting energy and angular spreads of the RNBs are much larger than those of a standard beam from an accelerator (by a factor of ten or more). In fact, the total emittance of secondary beams is determined by the combination of the nuclear reaction kinematics and atomic processes such as multiple angular scattering and energy loss straggling in the production target and in any degrader. The use of *profiled* degraders can reduce the emittance, for example, an achromatic degrader gives a factor of four, or so (Schmidt *et al*. 1987). The RNB

PHILOSOPHICAL TRANSACTIONS OF THE ROYAL SOCIETY A MATHEMATICAL, PHYSICAL & ENGINEERING SCIENCES

kinetic energy spread is also relatively large, of the order of several per cent, directly depending on the acceptance of the device, but can be observed in the flight time of the ions and corrected on an event-by-event basis or by using a *monokinetic* degrader from which all ions emerge with the same energy. A review of degrader shapes, uses and effects has also been published (Geissel *et al*. 1989).

The primary beam passes through the production target and retains a large fraction of its initial kinetic energy (*ca*. 90% or more). Therefore, an advantage of fast-ion separation techniques is that this production target only needs to be able to dissipate a fraction of the beam power. The unreacted beam is collected at some point in the separator itself. Radiation shielding is relatively simple since the volume of the reaction chamber can be kept relatively small. The particle identification of fast ions is also relatively simple, and the contaminant level can be easily checked on-line.

One final significant feature of in-flight separation is that the process is not sensitive to chemical properties or, in general, to the half-life of the RNB. Any limitation on the half-life is only given by the flight time of the ions through the device (almost always less than 1 μs, but longer, of course, in cooler rings). The net result is that, given suitable ion optics, the efficiency of the in-flight separation techniques can reach essentially 100%.

We discuss the general features of the reaction mechanisms that have been used to produce radioactive beams by in-flight separation in § 2. In § 3 we review the separation techniques used to purify the secondary beams. Some discussion is given on the possibilities for expansion of the techniques in new facilities. In § 4 we discuss some experimental techniques that can be used to overcome some of the problems associated with the poor emittance of these RNBs. In § 5 we present a short comparison of in-flight separation with ISOL techniques, and finally, in § 6 we offer some conclusions.

2. Production methods

(*a*) *Projectile fragmentation*

Projectile fragmentation was first identified in reactions of heavy ions with kinetic energies of the order of 200 MeV per nucleon or more (Goldhaber & Heckmann 1978; Hüfner 1985). The general features seem to remain at energies as low as 40 MeV per nucleon but probably not at 20 MeV per nucleon. The process involves a peripheral interaction of the projectile with a target nucleus in which some nucleons are removed and the residue undergoes a small recoil. Coulomb deflection and the nuclear recoil of the ion are small so that the large initial velocity can focus all the products into a narrow cone. The mass, charge, and velocity distributions of the products have been equally well described in a microscopic nucleon–nucleon scattering model or a macroscopic abrasion framework because all the models predict the creation of excited primary residues that must undergo statistical de-excitation (Morrissey *et al*. 1979). We will briefly describe the two models.

The intranuclear cascade model of proton-induced reactions was generalized to nucleus–nucleus collisions by Yariv & Fraenkel (1979, 1981). This model relies on assumptions that are valid above 100 MeV per nucleon, and follows the nucleon–nucleon scattering of the nucleons initially bound in the target and projectile, to predict many features of the collision. The computer model (ISABEL) gives somewhat narrow distributions of target and projectile residues that have high excita-

tion energies. A statistical de-excitation calculation is used to predict the observed ground-state nuclei. Fauerbach (1992) has coupled the ISABEL code to a modern statistical de-excitation code written by Gavron (1980) called PACE, and the predictions from the resulting program (ISAPACE) are remarkably good.

On the other hand, a macroscopic model based on the removal of nucleons in the volume eclipsed by the target and projectile and the subsequent de-excitation of the primary products has also been successful (J. D. Bowman and others, unpublished work; Gosset *et al*. 1977). This approach is called alternatively the participant–spectator model or the abrasion–ablation model. The target nucleus is imagined to shear off part of the projectile, leaving the rest of the projectile to travel forward at the initial beam velocity, with a minor downshift in velocity and some excitation energy. The primary residues (projectile or target) then undergo statistical de-excitation processes leading to the observed products (Morrissey *et al*. 1978). This model has been extended in terms of a more microscopic calculation of the excitation energy and the angular momentum of the residues by Schmidt and co-workers (Gaimard & Schmidt 1991; deJong *et al*. 1997).

A remarkable feature of the observed fragment cross-sections is that they are relatively constant from approximately 40 MeV per nucleon to 2 GeV per nucleon. The cross-sections are largest for fragments close in mass, but lower, than the initial nucleus and decrease exponentially with decreasing mass number. The isotonic distributions are nearly Gaussian and have a most probable neutron number that is significantly lower than that for stability. The near constancy of the production cross-sections allows simple empirical parametrizations of the existing cross-section data to make quite good estimates. For example, Sümmerer & Morrissey (1990) and Sümmerer *et al*. (1990) have generalized the parametrization of proton-induced reaction data by Rudstam (1966) to predict all projectile and target fragmentation cross-sections. The parameters were fitted to data taken from a wide range of target and projectile fragmentation studies and the overall agreement with many measurements is quite good. The parametrization is expected to be valid at high energy in which the cross-sections become constant, but a number of results measured at GANIL, MSU and RIKEN with beam energies in the range of 50–100 MeV per nucleon also agree with the predictions. The initial estimates of cross-sections needed to plan experiments are usually made with this parametrization and only small modifications have been suggested (Pfaff *et al*. 1996).

The cross-section of a given projectile residue only depends on the target through a geometrical factor in the high-energy limit of fragmentation reactions and only fragments that are lower in mass than the projectile are expected to be produced. However, nucleon transfer can be seen to play an important role at lower beam energies. First, a strong target dependence is observed for the production of nuclei far from stability. Very-neutron-rich nuclei are best produced with a heavy production targets (Mueller & Anne 1991) and proton-rich nuclei near the limit of stability are produced with the heavier $N \sim Z$ targets. For example, recent experiments to search for ^{69}Br from ^{78}Kr beams used ^{58}Ni targets (Blank *et al*. 1995; Pfaff *et al*. 1996). A few nuclei with atomic numbers greater than that of the beam were also observed in these experiments, as well as a few residues with $A = 79$ and 80. Neutron pickup products have also been observed in 80 MeV per nucleon ^{18}O reactions on ^{9}Be and ^{181}Ta targets at the NSCL (Souliotis *et al*. 1992) indicating that some cross-section is still present for few nucleon pickup at relatively high energies.

In addition to the production cross-section, the other key ingredient of the projectile fragmentation mechanism that determines the properties of the radioactive beam are the fragment momentum distributions. The momentum distributions directly determine the emittance of the fragment beams. The momentum distributions are characterized by a small downshift in velocity and a nearly Gaussian spreading that is larger than the downshift. In a very early study, Goldhaber (1974) showed that the momentum width of fragments created in a direct breakup process is related to the Fermi momentum of the removed nucleons. For the momentum parallel to that of the beam, one writes

$$\sigma_{\parallel} \quad [\mathrm{MeV}/c] = \sigma_0 \sqrt{\frac{A_\mathrm{f}(A_\mathrm{b} - A_\mathrm{f})}{A_\mathrm{b} - 1}}, \tag{2.1}$$

where σ_0 is a fraction of the mean Fermi momentum of the removed nucleons, A_b and A_f are the number of nucleons in the beam and fragment, respectively. The value of σ_0 should be approximately 100 MeV/c, based on electron scattering measurements, but the experimental data are better described by a value closer to 85 MeV/c (for beam energies over 40 MeV per nucleon), which is about 80–90% of the Fermi momentum. This difference can be explained as an effect of the Pauli principle which limits the number of nucleons which can participate (Bertsch 1981), although the predicted target dependence of this effect has not been reported. Given that excitation and decay plays an important role in these reactions, Morrissey (1989) has shown that the increase of the variance of the parallel momentum with the mass loss $(A_\mathrm{b} - A_\mathrm{f})$ is a general consequence of momentum conservation in the projectile rest frame for both direct breakup and statistical, sequential decay.

The parallel and perpendicular momentum distributions should be the same if nuclear and Coulomb scattering are small, that is, at high beam energies. At bombarding energies from 30 to 200 MeV per nucleon this description is apparently also valid, although the reaction mechanisms may not be as simple. However, it is true that the observed isotope and momentum distributions are very similar over a very large energy range. An important difference at low energies is that an orbital dispersion is present that adds a contribution to $\sigma_\perp$ (Van Bibber 1979). This contribution increases the perpendicular momentum width,

$$\sigma_\perp \quad [\mathrm{MeV}/c] = \sqrt{\sigma_\parallel^2 + \sigma_N^2}, \tag{2.2}$$

where σ_N was found to be approximately 200 MeV/c. The details of these momentum distributions have been studied and systematized (see, for example, Pfaff *et al*. 1995). The other important difference is that the momentum distributions are not fully Gaussian at low energies, and develop a low-energy tail. This low-energy tail can contribute significant background to secondary beams that are separated by strictly magnetic analysis.

Another interesting and potentially very useful feature of these reactions is that the nuclear spin of fragments produced at finite angles can be polarized and the polarization can be maintained through the analysis system. The polarization arises from the localization of the impact at the periphery of the nucleus and should be linked to the linear (parallel) momentum distribution. Asahi and co-workers showed that up to 20% of the ^{12}B fragments observed at 5° from a 40 MeV per nucleon ^{14}N beam were polarized (Asahi *et al*. 1990). Further, the amount and direction of the

polarization was correlated with the fragment momentum. The systematic behaviour of the polarization of the spin continues to be studied (Okuno *et al*. 1994) and could be very useful for radioactive beam studies.

Although a considerable amount is known about peripheral reactions in the 30 MeV per nucleon to 2 GeV per nucleon range, there are still important aspects about the reaction mechanism to study. An interesting question for the production of nuclei very far from stability is whether these simple descriptions are valid for nuclei produced at the limits of stability. For example, the 'fragile' nucleus ^{11}Li is produced at rates that are consistent with the systematics for production of (much) more stable nuclei. Presumably, the fragile nuclei must be formed in relatively cold processes, yet the models predict that the fragmentation process is not, in general, cold. Other aspects of the reactions, such as the role of dissipative and transfer processes below 200 MeV per nucleon and the reduction of σ_0 from the value consistent with the internal Fermi momentum, are not fully understood.

(*b*) *Projectile fission*

Although projectile fragmentation is used to produce light neutron-rich nuclei, the maximum yield of projectile fragmentation products is obtained for neutron-deficient nuclei. On the other hand, nuclear fission has been an extremely important source of neutron-rich nuclei for a long time. Bernas and co-workers have shown that the fission of very energetic uranium beams can be used to produce and study a range of neutron-rich nuclei that had not been studied before (Bernas *et al*. 1994, 1997).

The fission process creates nuclei with a kinetic energy of approximately 1 MeV per nucleon and the angular distribution of products is essentially isotropic for low values of angular momentum. Thus, the recoil vectors of the products are distributed on the surface of a slightly diffuse sphere. If the fissioning nucleus is moving with a kinetic energy that is large compared to the fission recoil, then the products can be collected efficiently and separated by using in-flight techniques similar to those used for projectile fragments. However, only one or the other kinematic solution, e.g. forward going in the rest frame, can be accepted by present separators. The high energy also limits the number of atomic charge states of the products and the unreacted beam. Recently, it has been shown that the fission of significantly slower nuclei can be used to make similar neutron-rich nuclei (Souliotis *et al*. 1997) but in this case the kinematic focusing is less and the large number of charge states of the beam severely complicates the separation. With these limitations the fission of very energetic projectiles is an important process for the production of neutron-rich nuclei, due to the lack of other methods to produce these nuclei.

(*c*) *Direct reactions*

Direct or simple transfer reactions are highly selective and can produce specific nuclei in specific states with reasonable cross-sections and are complementary in a way to fragmentation processes. Direct reactions have been used at low energies to produce radioactive beams, examples include Osaka University (Yamagata *et al*. 1989), the Lawrence Livermore National Lab (LLNL) (Haight *et al*. 1983), and Notre Dame University (Kolata *et al*. 1989; Becchetti *et al*. 1991). Direct reactions often have large cross-sections and narrow angular distributions that can be used to convert

PHILOSOPHICAL TRANSACTIONS OF THE ROYAL SOCIETY A MATHEMATICAL, PHYSICAL & ENGINEERING SCIENCES

a significant fraction of the beam into a single product in a specific nuclear state. Even for primary beams with several hundred megaelectronvolts per nucleon the transfer cross-sections for single nucleon transfer can be tens of millibarns per steradian near zero degrees.

A particular advantage of using direct reactions is that the secondary beam energy spread can be kept very small in those cases in which only one final state is populated. The secondary beam energy spread is then determined by the thickness of the production target. If a low mass target can be used, such as H_2, in a single nucleon transfer reaction, e.g. (p,d), the forward focusing of the 'reverse kinematics' creates a factor of 10 or more compression of the CM angles when transformed into the laboratory. It may be possible to produce beam intensities of up to 10^9 radioactive ions per second with this technique, although it will be limited to specific nuclei near stability.

(*d*) *Coulomb dissociation*

The process of low-energy Coulomb excitation of stable beams has been used to study low-lying excited states. At higher beam energies, the equivalent photon flux present as a fast ion moves past a heavy target is so large that the excitation of the giant dipole resonance (GDR) becomes very important (Bertulani & Baur 1988). Nuclei excited into the GDR primarily decay by neutron emission and produce a nucleus with one less neutron than the (stable) beam. For example, the electromagnetic dissociation cross-sections are several barns for the reaction of heavy nuclei with heavy targets for kinetic energies of the order of gigaelectronvolts per nucleon (Mercer *et al*. 1986; Hill *et al*. 1988).

The secondary beams formed by Coulomb dissociation would have energy and angular widths that depend only on the decay energy of the neutron from the GDR which is approximately $77/A^{1/3}$ MeV. For very heavy beams (of order 1 GeV per nucleon) the recoil spreading is a small effect. In principle, beams of specific heavy nuclei, near to stability, could be produced with good emittances and with beam intensities of more than 10% the primary beam intensity.

3. Separation techniques

As mentioned in the Introduction, it appears that the optimum separation device for fast projectile residues is a momentum-loss achromat. Electric fields and solenoidal magnets are also useful for kinetic energies below 100 MeV per nucleon or so. The present discussion will concentrate on describing the momentum-loss achromat technique (Schmidt *et al*. 1987; Geissel *et al*. 1989, 1995) and the intensities that are possible with these devices. The use of solenoidal magnets will be briefly described in § 3 *c*.

(*a*) *Fragment separation with profiled degraders*

The term *achromatic* is used in practice to mean that the horizontal position of a particle at the end of the separator does not depend on its momentum. Achromatic systems have the advantage that the final spot size is kept small even when the momentum acceptance is large. Figure 1 illustrates the basic ion-optical concepts of

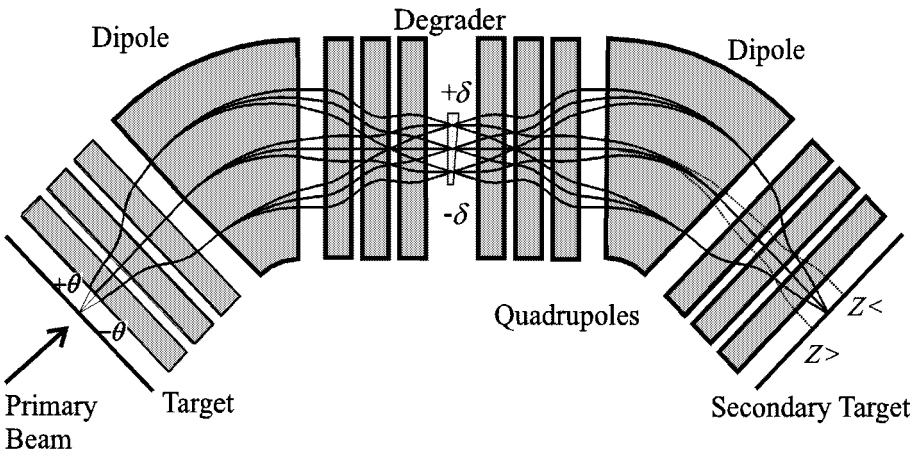

Figure 1. Schematic illustration of the ion-optical trajectories used in the momentum loss achromatic technique.

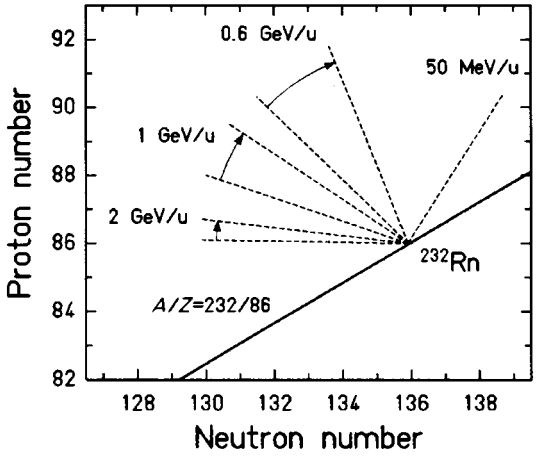

Figure 2. Illustration of the effects of the two selections made in a momentum-loss achromat, taken from Schmidt *et al.* (1987) The solid line represents the effect of the first bend that selects according to A/Z. The second selection, represented by the dashed lines, is determined by the $B\rho$ change of each ion after passing though the degrader. The second selection is velocity dependent.

fragment separation in a momentum-loss achromat. The ion trajectories for different momenta and initial scattering angles of the same isotope are indicated by the lines in the figure. Note that the ions are focused to a small spot at the focal plane of the device, independent of the initial angle or momentum. The key elements in the device are an initial bend for momentum-to-charge ratio selection, an energy loss degrader for atomic number separation also called a 'wedge', and a second bend for momentum-to-charge ratio selection of a specific ion. (We will assume that all the ions are fully stripped for the moment.)

An aperture or a slit is used at the intermediate position to limit the momentum acceptance of the device. Since the fragmentation mechanism produces nuclei at nearly the same velocity, the initial $B\rho$ or momentum-to-charge ratio selection

is equivalent to mass-to-charge ratio separation. Even so, projectile fragmentation reactions can produce many different ions that have the same mass-to-charge ratio, e.g. the fragmentation of an ^{18}O beam will produce five ions with $m/q = 3$: ^{3}H, ^{6}He, ^{9}Li, ^{12}Be, and ^{15}B. An energy degrader is inserted into the beam at the intermediate dispersive image in order to remove the ions that have the same initial mass-to-charge ratio as the fragment of interest but different atomic number (Z). The ions will lose different momenta in the degrader depending on their atomic number and will exit the foil with different magnetic rigidities. The contaminants can then be dispersed at the focal plane by an additional bend. This Z-dependent separation is proportional to the degrader thickness and to the ratio of the magnetic rigidity of the second half of the system to that of the first half (Schmidt *et al*. 1987). The effect of this selection procedure is shown schematically in figure 2, taken from Schmidt *et al*. (1987). The first $B\rho$ selection makes a cut according to A/Z and the second $B\rho$ selection acts on the distribution of velocities created by the energy loss. The velocity dependence of the second selection is also shown in the figure. The variations in the slopes of the selections in the second half were found by varying the thickness of the degrader from 0 to 80% of the ion's range.

An example of how well the technique works is shown in figure 3, taken from Geissel *et al*. (1992*a*), in which the separation of ^{188}Pt ions from the fragmentation products of a 1 GeV per nucleon ^{208}Pb beam was measured and compared to a calculation with the MOCADI code (Schwab 1992). The contours are shown for the ion intensities as a function of position at the end of the FRS, labelled F_4, versus their position at the midpoint of the device, labelled F_2. Proper adjustments of aperture slits at F_2 and F_4 allow single individual isotopes to be selected. The left panel of the figure shows the measured data and the right panel shows the simulation with the computer code MOCADI.

The mass-resolving power of a fragment separator can be expressed to first order as

$$R_{\mathrm{mass}} = \frac{(x/\delta)_1}{(x/x)_1 x_0} \frac{(\delta/\delta_m)}{(\delta/\delta_0)}, \tag{3.1}$$

where $(x/\delta)_1$ is the dispersion of the first set of dipoles, $\delta = (p - p_0)/p_0$ is the percentage momentum deviation from the central momentum, $\delta_m = (m - m_0)/m_0$ is the percentage change in the momentum caused by a percentage change in A at the degrader with the charge held constant, x_0 is the initial spot size, and $(x/x)_1$ is the magnification at the dispersive image. In each case, the subscript 0 denotes the value for the central ray. A very similar expression can be written for the charge-resolving power,

$$R_{\mathrm{charge}} = \frac{(x/\delta)_1}{(x/x)_1 x_0} \frac{(\delta/\delta_z)}{(\delta/\delta_0)}, \tag{3.2}$$

where $\delta_z = (z - z_0)/z_0$ is the percentage change in the momentum caused by a percentage change in Z at the degrader with the mass and momentum held constant. Equations (3.1) and (3.2) are valid for an achromatic system with

$$(x/\delta)_2 = -(x/x)_2 (x/\delta)_1 \tag{3.3}$$

and a degrader shaped to preserve the achromatism (achromatic degrader). The important point to notice is that the first term in both equations for the resolution is

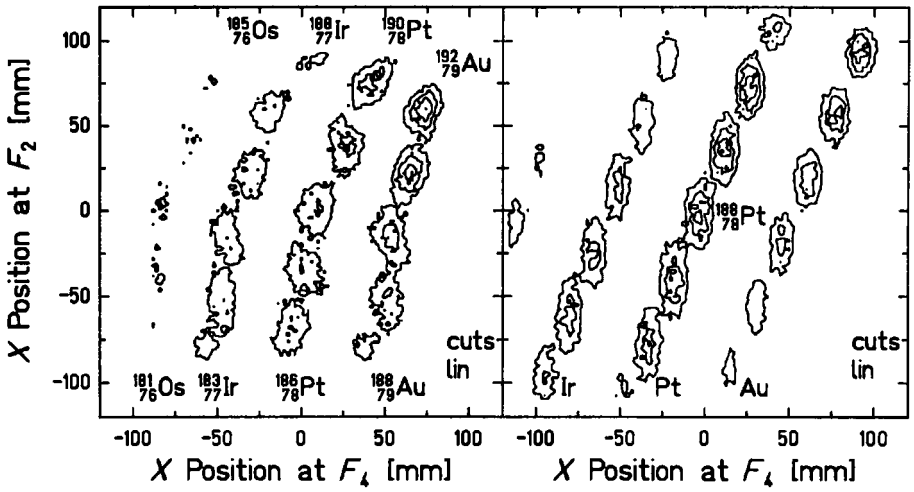

Figure 3. The calculated separation of ^{188}Pt produced by fragmentation of a 1 GeV per nucleon ^{208}Pb beam. The horizontal distribution of each ion at the end of the FRS, F_4, versus its position at the midpoint, F_2 is shown for the measured data on the left and for the computer simulation on the right. This figure is taken from the work of Geissel *et al*. (1992*a*) with the calculations were performed with the program MOCADI (Schwab 1992), which starts from the nuclear cross-sections convoluted in the distributions (Sümmerer & Morrissey 1990; Sümmerer *et al*. 1990).

simply the momentum-resolving power of the first half of the system. Hence, a lower momentum-resolving power implies a less pure secondary beam. For mass-resolving powers of the order of 200, the intrinsic momentum-resolving power of the device should be 1000 or greater. This requirement has important consequences for the design of the separator and indicates that the emittance of the primary beam should be as small as possible in order to reduce the spot size, x_0, and thus increase the resolving power. Also, as discussed in § 4 *b*, the emittance of the secondary beam is determined by the initial beam spot size. We should note that, in general, it is not necessary to use degraders with achromatic profiles. An alternative approach is to use a homogeneous degrader and tune the magnetic system of the second half to match the dispersion of the beam after the degrader.

The achromatic separator technique has been implemented in several laboratories around the world that can provide a wide variety of relatively high-energy primary beams. As noted in the Introduction, there are separators operating in Germany, France, Japan and the United States. Other similar devices are in the planning stages or are under construction. Figure 4 shows a world view of operating and planned separators. Laboratories such as GANIL, MSU and, at one time, LBL have more than one separation facility. A comparison of the various parameters that describe the fragment separators is given in table 1. The LISE separator has been operated for more than 10 years and has provided beams for a variety of experiments. The RIPS device had the largest solid angle and momentum acceptance of operating devices, but the recently constructed COMBAS device at the JINR at Dubna will have a significantly larger acceptance. The large horizontal acceptance of 80 cm of COMBAS is achieved by using high index dipoles. This is a novel design which has many attractive features. The A1200 and A1900(MSU), RCNP(Osaka), and FRS(GSI)

Table 1. *Comparison of fragment separators*

device	Ω (msr)	$\Delta p/p$ (%)	$B\rho$ (T m)	resolving power	length (m)	reference
A1200	0.8–4.3	3.0	5.4	700–1500	22.0	Sherrill 1992
A1900	8.0	4.5	6.0	*ca.* 2900	35.0	Morrissey 1997
COMBAS	6.4	20.0	4.5	4360	14.5	Artukh *et al.* 1993
LISE	1.0	5.0	3.2	800	18.0	Mueller & Anne 1991
FRS	0.7–2.5	2.0	9.0–18.0	240–1500	73.0	Geissel *et al.* 1992*a*
RIPS	5.0	6.0	5.76	1500	21.0	Kubo *et al.* 1990
RCNP	1.1	8.0	3.2	2000	14.8	Shimoda *et al.* 1992
Notre Dame	33.0	15.0	0.54	50	1.8	Kolata 1989
MARS	9.0	var.	1.79	300[a]	19.0	Tribble *et al.* 1989

[a]Mass-to-charge resolution, see the text.

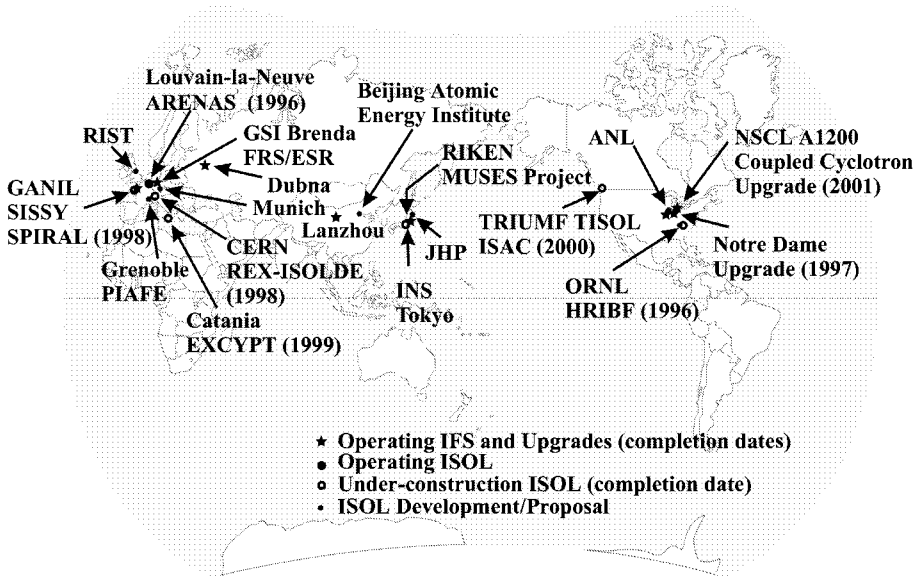

Figure 4. World view of fragment separators that are operating (marked with a star), that are planned or are under construction (marked with a circle).

separators are positioned at the beginning of the beam distribution system to allow delivery of radioactive beams to any experimental area. The GSI device has been designed for very high kinetic energies, where the fragmentation cone and relative energy spread are smaller and therefore allow the physical acceptance of the device to be smaller.

Besides the obvious dependence of the RNB intensity on the intensity of the primary beam, the secondary beam rate is also directly related to the relative separator acceptance. Large solid angle and large momentum acceptance are especially important if the device is to be used to separate light ions at 50–200 MeV per nucleon. Notice that the larger the acceptance the separator, the lower the primary beam energy can be to reach 100% collection efficiency.

Table 2. *Beam intensity estimates*

(Estimates of the secondary beam intensities from the program INTENSITY. The production target was ^{9}Be metal with the thickness specified in g cm^{-2}. The beam intensity was taken to be 1 pμA for all beams except Cd and Sn which were assumed to be 0.1 pμA, the primary beam energy was 400 MeV per nucleon.)

beam	fragment	target (g cm^{-2})	σ_S (mb)[a]	rate (pps)	σ_G (mb)[b]	rate (pps)
^{7}Li	^{6}He	18.2	13.4	1.9×10^{10}	20.0	2.8×10^{10}
^{11}B	^{8}He	10.5	0.05	5.2×10^{7}	0.5	5.3×10^{8}
^{14}C	^{11}Li	9.5	0.01	1.5×10^{7}	0.1	1.4×10^{8}
^{20}Ne	^{19}Ne	13.8	20.3	4.6×10^{10}	65.6	1.5×10^{11}
^{106}Cd	^{104}Cd	5.0	2.7	2.3×10^{8}	28.0	2.4×10^{9}
^{112}Sn	^{100}Cd	4.4	0.05	4.1×10^{6}	0.05	4.1×10^{6}

[a]Based on cross-sections calculated with the parametrization of Sümmerer & Morrissey (1990) and Sümmerer *et al*. (1990).
[b]Based on measured cross-sections or trends for the same number of removed nucleons from the data of Webber *et al*. (1990).

(*b*) *Radioactive beam intensities*

For the purposes of illustration, we have calculated the intensities for a variety of secondary beams. The choice of ions was arbitrary but indicates the range of nuclei that have been used in recent nuclear physics experiments. The projectile fragmentation process is the most general mechanism for producing such a wide variety of beams and the properties of projectile fragments, discussed above, have been used in our estimates. The estimation process must include production in a target of given thickness including the nuclear scattering effects and atomic effects such as differential energy loss and straggling. After leaving the target we only consider the acceptances of the device and atomic effects in the energy degrader. A simulation program called INTENSITY (Winger *et al*. 1992) was developed in order to keep track of all of these effects and provide estimates of the secondary beam rates. This code can also help evaluate the optimum bombarding energy, target thickness, usefulness of various profiled degraders, and so on. The code also includes an empirical treatment of the charge state distributions that was not used here but is extremely important at lower bombarding energies.

Table 2 gives a few examples of the secondary beam intensities expected from a hypothetical fragment separator with a solid angle of 5 msr and a momentum acceptance of 6%. These parameters are typical of the larger values of the devices listed in table 1. The primary beam intensity was taken to be 1 pμA unless noted, a value that is also large but not unrealistic. The target thickness was chosen to maximize the RNB rate. The beam energy was assumed to be 400 MeV per nucleon so that the relative acceptance of the device was quite high. In fact, no significant increase in intensity was found for the cases listed if the primary beam energy was raised to 800 MeV per nucleon (in part a consequence of the large acceptance of the separator). The production cross-sections were taken from the data of Webber *et al*. (1990), or estimated from trends in that data, and from the parametrization of Sümmerer & Morrissey (1990) and Sümmerer *et al*. (1990).

The values of the secondary beam intensities are quite substantial, ranging up to 10^{10} particles per second. We also note that the cross-section estimates are relatively close, within a factor of two or so. A similar level of agreement between measured and predicted rates is typical.

(c) *Solenoidal magnets*

An alternative in-flight separation technique which has been very successful uses a solenoid magnet as a large-solid-angle collector. Radioactive beams have been produced and used at Notre Dame University (NDU) (Kolata *et al*. 1989; Becchetti *et al*. 1991; Becchetti & Kolata 1997). This work uses few nucleon transfer reactions at 1–3 MeV per nucleon to produce beams in the 10^2–10^7 range. The primary beam rejection is excellent and other contaminants are identified with Silicon E, ΔE telescopes. A second-generation system is being completed at NDU that will use two magnets, each producing a maximum magnetic field of about 6 T. A solenoid will be added to the beamline at the ATLAS facility at Argonne National Lab in order to improve the acceptance of secondary beams. A larger solenoid has been used at the NSCL with heavy ions at higher energies, up to 50 MeV per nucleon (O'Donnell *et al*. 1994). A related project is also underway at GANIL to use superconducting solenoids to increase the beamline transmission of fragmentation products, discussed below (Joubert *et al*. 1991).

The solenoidal devices are at once simple and limited. They allow a large solid angle for collection and a symmetric acceptance. However, the separation effectiveness is limited to lighter beams. The double solenoid system at NDU will allow greater flexibility. The double solenoid device at GANIL is primarily used to provide an extremely small beam spot on target and the fragments are then separated by magnets in the beam transport system, see below. In general, if the secondary beam energy is low enough, solenoids offer an efficient means of collection of secondary products.

4. Experimental techniques

We now turn to a brief discussion of the techniques that have been developed to overcome some of the limitations in the beam quality of fast secondary beams. We will specifically focus on the beams produced by projectile fragmentation and separated by the momentum-loss achromats. The major drawbacks of beams produced by projectile fragmentation are: (1) poor longitudinal and transverse beam emittance arising from the primary nuclear reaction and the acceptance of the device, (2) beam energies that are much higher than those required in the secondary experiments, and (3) the level of impurity when the resolving power of the separator is not sufficiently high. These disadvantages can be overcome in most cases, depending on the exact needs of the secondary experiment.

The transverse secondary beam emittance is given approximately by

$$\epsilon_0 = x_0 \times \Delta\theta \quad [\text{mm mr}], \tag{4.1}$$

where x_0 is the production target spot size, and the angular spread is given by the maximum of the separator acceptance or by the nuclear reaction,

$$\Delta\theta = \sigma_\perp \times 2.35/p_\parallel, \tag{4.2}$$

where $p_{\|}$ is the average parallel component of the ion's momentum. Since $\Delta\theta$ is determined by the production mechanism, as discussed in § 2 *a*, the only ways to reduce the beam emittance are to reduce x_0 or to limit the angular acceptance of the device (which lowers the secondary beam intensity).

Two systems have been developed to reduce the spot size of the primary beam and improve the emittance and yield of secondary fragments. A pair of superconducting solenoids was built at GANIL to surround a high-intensity target (SISSI system) at the exit of the second cyclotron and before the alpha-spectrometer (Joubert *et al.* 1991). The first solenoid is used to produce a very small beam spot, $x_0 \approx 0.2$ mm, by acting as a strong demagnifying lens. The second solenoid collects the large angular spread of the fragments. The resulting secondary beam emittance can be more efficiently transported to experimental areas even though the acceptance of the beam lines is quite small. A magnetic quadrupole doublet was installed just before the target position of the A1200 separator at MSU for similar purposes. The spot size in this case is $x_0 \approx 1$ mm, and has provided an improvement in emittance of about a factor of four and subsequently a similar factor in transmitted beams to experiments.

Those secondary experiments that require beam energies which are well below the optimal (or lowest reasonable) production energy can be performed by decelerating the secondary beam. Brute force deceleration in an energy degrader has been performed in many cases, but the beam emittance usually grows so large that only a fraction of the secondary beam is useful; see below. The beam should be 'cooled' to maintain a reasonable secondary beam emittance during the deceleration process. The GSI has built a large ring-system with such capabilities, called the ESR. The effectiveness of cooling RNBs was first demonstrated by Geissel *et al.* (1992*b*). This technique was applied to measure the half-lives of isomeric states by Irnich *et al.* (1995) and more recently in a systematic measurement of a broad range of masses (Geissel 1997; Wollnik *et al.* 1997).

Two other much more sophisticated ring-systems have been proposed. The JINR in Dubna has proposed the K4-K10 system (Gorshkov *et al.* 1993), and RIKEN has proposed building the imposing MUSES system (Tanihata 1997). At the facility proposed in Dubna, the first ring, labelled K4, is used to stack and cool primary beam to achieve a very small beam emittance. This allows small production beam spots and hence relatively good secondary beam emittance, as in the SISSI project. This technique also limits the emittance which must be accepted in the second ring, labelled K10. A fragment separator would be located between the K4 and K10 rings, and serve as the injection line into the larger ring. The second ring would be used to cool, accelerate, or decelerate the secondary beams. The MUSES system is proposed to consist of four rings to collect, store and react, and accelerate secondary beams produced at a few hundred megaelectronvolts per nucleon. The first ring will be an accumulator–cooler ring (ACR), followed by a double storage ring (DSR), and finally a booster synchrotron ring (BSR). The ACR will store and cool the beams produced in a very large fragment separator (Big-RIPS) in order to produce a low-emittance high-intensity RNB. The cooled beam will be either transported to the storage ring and or the booster ring, or used in nuclear physics and/or atomic physics experiments directly. The DSR will have the very unusual feature of being able to store electron beams as well as radioactive beams. Therefore, the DSR will allow electron-RNB scattering experiments for the first time. Finally, the BSR will be able to boost the energy of the RNB from the ACR (or the electron beam) before injection into DSR.

A fundamental limitation of beam cooling is that the amount of time necessary to store and cool the ions is of the order of seconds, and hence ions with a very short half-life will decay. During deceleration, the intensities are expected to be reduced by at least an order (and typically two orders) of magnitude, mainly due to: limitations in the number of nuclei which can be cooled, space charge limitations, pulse structure matching, and in some cases the time necessary for deceleration. Such techniques, however, appear feasible and are being explored at GSI. The typical intensities of ions decelerated to the Coulomb barrier would probably be in the range of 10^6–10^7 ions per second and some of the difficulties would not be present for these weaker beams.

Decay-spectroscopy experiments have the simplest requirements in that the RNBs are generally stopped in a catcher. Stopping gigaelectronvolt-per-nucleon ions in a thin collector is not easy because the ranges are very long. If electromagnetic dissociation of the ions can be neglected, then a heavy stopping material is best, in order to keep the number of secondary interactions low. The range straggling of secondary ions can be minimized by using a monokinetic degrader rather than the standard achromatic wedge (Geissel *et al*. 1989). In this case, the limit is set by the momentum resolution of the device and energy loss straggling. Geissel *et al*. (1989) have calculated the effectiveness of the monoenergetic wedge technique for stopping ^{20}Ne ions. The range straggling limit is only 10% larger than that for a monoenergetic ^{20}Ne primary beam with the same central kinetic energy as that of the degraded beam.

A difficulty with this technique is that during the slowing down process the transverse emittance grows by essentially the ratio of the momentum spread entering the degrader to the momentum spread exiting the degrader (Schmidt *et al*. 1987). Hence, large momentum compression factors lead to large transverse emittances. This energy compression technique has been used by Matsuta *et al*. (1992) at LBL to slow down and collect ^{43}Ti ions produced from a 214 MeV per nucleon ^{46}Ti primary beam. The ^{43}Ti ions were slowed and compressed to $\pm$1.5 MeV per nucleon just before stopping. Similar compression techniques are being considered for medical applications with beams that have large momentum spreads.

A related difficulty with secondary beams from achromatic separators is their large longitudinal emittance or momentum spread. The width, σ, of the momentum distribution is given by equation (2.2) combined with the momentum acceptance of the fragment separator. For example, the full momentum acceptance (3%) of the A1200 device at MSU is generally filled by the reactions used to produce low-mass products. Such a large energy spread in the secondary beam would make spectroscopic experiments, such as transfer reactions with the RNBs, difficult.

Two approaches have been used to alleviate this problem. First, the fragment separator itself can be used as an energy-loss spectrometer. This technique was used with the A1200 to measure a variety of parallel momentum distributions from the breakup of halo nuclei (Orr *et al*. 1992; Kelley *et al*. 1995). This dispersion matching technique has also been used for charge exchange studies of mirror nuclei (Steiner *et al*. 1996) and for studying the (p,n) reaction with a ^{6}He beam in reverse kinematics (Brown *et al*. 1996). In all these cases a momentum resolution of 1 part in 1000 or better was achieved despite a 3% momentum spread in the secondary beam. Figure 5 shows the distribution of ^{3}He nuclei after the charge exchange by using a secondary ^{3}H beam at 125 MeV per nucleon that illustrates this technique. In this

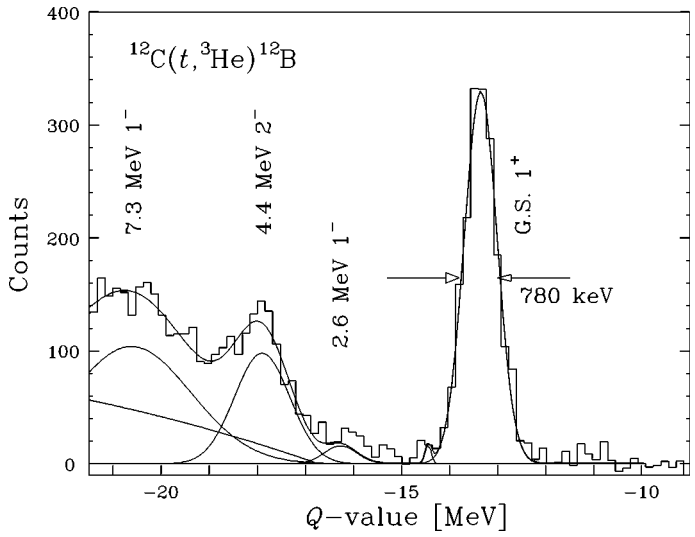

Figure 5. Results from an experiment with the A1200 fragment separator illustrating the energy loss mode. Despite a large momentum spread in the secondary triton beam, the ^{12}C(t,^{3}He) charge-exchange reaction was accurately measured by dispersion matching.

case, the momentum resolution was limited to about 1/1000 by the incoherent beam spot size, which was in turn dominated by the thick production target (Daito *et al*. 1998). The energy resolution was 750 keV despite the fact that the initial triton energy distribution was essentially flat with a 6% energy width (corresponding to 22 MeV).

The second approach to dealing with the large energy spread in the beam relies on measurement of the time-of-flight (TOF) for each ion over a large distance. An extreme example of this procedure is the TOF mass measurements by Orr *et al*. (1991). In this case the flight time was measured through a 82 m beamline in order to achieve a velocity resolution of 2.5×10^{-4}. By simultaneously measuring known masses, an energy resolution of 5.0×10^{-4} was achieved. In general, it may not be necessary to measure the flight times ion by ion. The arrival of the reaction products at a detector relative to a timing reference taken from the primary accelerator, such as the RF from a cyclotron, will provide a relative measurement of the ion's energy at the 1% level, depending on the path length and beam pulse structure.

Further uses of the ion's TOF are to identify contamination in the secondary beam and to remove unwanted events. TOF identification at the NSCL is often used with deliberately mixed or contaminated secondary beams. The time of flight of each ion relative to the cyclotron RF signal, or a plastic scintillator placed in the beamline, combined with an energy loss measurement, provides a clear identification of each ion, allowing discrimination among beam components.

5. Comparison with the ISOL technique

A question that commonly arises in the discussion of the production of secondary beams is 'What is the best technique to produce a certain beam?' The two production schemes that are compared are in-flight separation; and production by the

bombardment of thick targets with very-high-intensity proton (or other light ions), referred to as the ISOL technique. These two techniques are complementary in a way, since they use the same nuclear reaction mechanism, but in one case the residues come from the projectile (rapidly moving in the laboratory frame), and in the other, the residues come from the target (nearly at rest in the laboratory frame).

The production rate of secondary ions from an ISOL-type ion source (assuming that most beam particles do not interact) can be written,

$$R_{\mathrm{ISOL}} = \frac{I_{\mathrm{beam}}\sigma_{\mathrm{f}} t N_{\mathrm{A}}}{A_{\mathrm{t}}}\epsilon, \tag{5.1}$$

where I_{beam} is the proton beam intensity in particles per second, σ_{f} is the fragment production cross-section in cm^2, t is the target thickness in $\mathrm{g\,cm}^{-2}$, N_{A} is Avagodro's number, and A_{t} is the production target atomic mass in $\mathrm{g\,mol}^{-1}$. The ion source efficiency is given by ϵ and has a very high degree of variability. The production rate from heavy ion fragmentation reactions is similar,

$$R_{\mathrm{PF}} = \frac{I_{\mathrm{HI}} N_{\mathrm{A}} \sigma_{\mathrm{f}}}{A_{\mathrm{t}}(\mu_{\mathrm{b}} - \mu_{\mathrm{f}})}(\mathrm{e}^{-\mu_{\mathrm{b}} t} - \mathrm{e}^{-\mu_{\mathrm{f}} t}), \tag{5.2}$$

where I_{HI} is the heavy ion (HI) beam intensity, $\mu_{\mathrm{f(b)}}$ is the fragment (or beam) attenuation length in the production target, and the collection efficiency is assumed to be close to one. If the beam and fragment have the same attenuation length (for example, as is approximately the case for ^{11}C and ^{12}C) then equation (5.2) can be simplified to

$$R'_{\mathrm{FRS}} = \frac{I_{\mathrm{HI}} N_{\mathrm{A}} \sigma_{\mathrm{f}}}{A_{\mathrm{t}}} t \mathrm{e}^{-\mu_{\mathrm{f}} t}, \tag{5.3}$$

in which case the target thickness is limited to be in the order of the interaction length of the ions. This equation is actually a lower limit to the rate, since other secondary ions will interact and may produce the fragment of interest. For fragments that are far from stability, there is certainly an enhancement in their production rate in thick targets. Equation (5.3) is probably more valid for fragments closer to the beam.

If we assume that the product of the production cross-section and target thickness (in atoms per cm^2) are the same for both methods, then the ratio of rates is

$$\frac{R'_{\mathrm{PF}}}{R_{\mathrm{ISOL}}} = \frac{I_{\mathrm{HI}}}{I_{\mathrm{p\ beam}}} \frac{\mathrm{e}^{-\mu_{\mathrm{f}} t}}{\epsilon}. \tag{5.4}$$

The assumption of similar target thickness is justified if a hydrogen target is used for the projectile fragmentation reaction, in which case the two nuclear reactions are identical in the rest frame of the heavy nucleus. (For heavy ions moving through light targets the nuclear interaction length is shorter than electronic stopping length.) The cross-section assumption is also approximately true for heavier targets, since the fragmentation cross-section increases for higher mass targets (cf. Sümmerer & Morrissey 1990; Sümmerer *et al*. 1990). The projectile fragmentation cross-section to produce a specific secondary beam may actually be higher because the best possible stable isotopic beam can be used to produce a given fragment, whereas the ISOL facility is generally limited to certain target materials.

In considering equation (5.4), it is clear that ISOL facilities have the big advantage of high proton fluxes. The proton beam intensities can be of the order of 10^{14} while

heavy ion beam intensities are of the order of 10^{13} for light ions and decrease by up to two orders of magnitude for the heavier ions. This factor strongly favours the ISOL technique for raw-rate considerations.

The last factor in equation (5.4) is the ratio of the efficiencies of the two techniques and is essentially determined by the nature of the ISOL beam. This factor favours heavy ion production by 1.5 or so for alkali ions (the best ISOL beams), and grows to factors of 1000 or more for those ISOL beams with short half-lives or those that are difficult to separate chemically. Hence, for nuclei with short half-lives, or that are chemically stubborn elements, in-flight separation can provide higher rates despite the large difference in primary beam intensities.

Notice that ISOL beams must also be reaccelerated and HI beams must be slowed, depending on the needs of the secondary experiment. The losses may be similar in either case, but clearly if the fast HI beams can be used or are desired, they present an advantage over ISOL beams, which must be accelerated to above 10 MeV per nucleon, in which case an additional acceleration efficiency and the accelerator cost must be taken into account.

Fast HI fragment beams have the serious disadvantage of poor emittance and large energy spreads in most cases. As discussed, experiments can compensate for these effects, but become more complicated. In addition, if the in-flight fragments are stopped, depending on the fragment energy, the range can be very large and it is possible that the once pure fragments will interact in the stopper and add background. The poor emittance also makes the produced source sizes large and might complicate decay measurements. Such problems are not present for ISOL beams which have been used to make sources at low energy and with acceptable source sizes. The accelerated beams will have energy spreads and emittance which are a factor of 10 or more smaller than the fast HI fragment beams.

Finally, the purities of the beams can be expected to be equivalent. The requirement to achieve this level of separation is a fragment separator with sufficient momentum-resolving power. For ISOL beams, a high resolving power mass separator is also required. In the end, both techniques are complementary. The ISOL technique provides better quality, low-energy beams of nuclei nearer to stability, while the in-flight techniques provide beams of the shortest-lived and chemically difficult elements at higher energies.

6. Conclusion

In-flight separation of projectile fragments is a very general and useful technique for producing high-intensity radioactive beams. Momentum-loss achromat devices have been used to separate reasonably pure secondary beams. Just from the number of such facilities that are operating or are under construction, this technique can to be seen to have made a significant impact on radioactive beam physics. The advantages of this technique are fast separation, no chemical selectivity, relatively simple production targets, and beams which do not need reacceleration. There is also the advantage that almost any beamline with dipoles can be used as a fragment separator. The disadvantages are that the optimum production energies are often above the desired beam energies for secondary experiments, the poor emittance of the beam, and the limited intensity of primary beams. However, depending on the exact requirements of the RNB experiments, many of these difficulties can be overcome.

PHILOSOPHICAL TRANSACTIONS OF THE ROYAL SOCIETY A MATHEMATICAL, PHYSICAL & ENGINEERING SCIENCES

References

Alonso, J. 1984 *Proc. of the Workshop on Research with Radioactive Beams*. Lawrence Berkeley Laboratory Report LBL-18187. Washington, DC.

Alonso, J., Chatterjee, A. & Tobias, C. A. 1978 *IEEE Trans. Nucl. Sci.* **NS-26**, 3003.

Anne, R., Bazin, D., Mueller, A. C., Jacmart, J. C. & Langevin, M. 1987 *Nucl. Instrum. Meth.* A **257**, 215–232.

Artukh, A. G., and 28 others 1993 In *Proc. 3rd Int. Conf. on Radioactive Nuclear Beams* (ed. D. J. Morrissey), pp. 45–48. Gif-sur-Yvette: Editions Frontières.

Asahi, K. (and 14 others) 1990 *Phys. Lett.* B **251**, 488–492.

Becchetti, F. D. & Kolata, J. J. 1997 In *Proc. 14th Int. Conf. on Applications of Accelerators in Research and Industry, November 1996*. Denton: AIP Press.

Becchetti, F. D. (and 10 others) 1991 *Nucl. Instrum. Meth.* B **56/57**, 554–558.

Bernas, M. (and 20 others) 1994 *Phys. Lett.* B **331**, 19–24.

Bernas, M. (and 20 others) 1997 *Nucl. Phys.* A **616**, 352c–362c.

Bertsch, G. 1981 *Phys. Rev. Lett.* **46**, 472–473.

Bertulani, C. A. & Baur, G. 1988 *Phys. Rep.* **163**, 299–408.

Blank, B. (and 17 others) 1995 *Phys. Rev. Lett.* **74**, 4611–4614.

Brown, J. A. (and 12 others) 1996 *Phys. Rev.* C **54**, R2105–R2108.

Daito, I. (and 22 others) 1998 *Nucl. Instrum. Meth.* A **402**, 177–181.

Davids, C. N. & Larson, J. D. 1989 *Nucl. Instrum. Meth.* B **40/41**, 1224–1228.

deJong, M., Ignatyuk, A. V. & Schmidt, K.-H. 1997 *Nucl. Phys.* A **613**, 435–444.

Dufour, J. P., del Moral, R., Emmermann, H., Hubert, F., Jean, D., Poinot, C., Pravikoff, M. S., Fleury, A., Delagrange, H. & Schmidt, K. H. 1986 *Nucl. Instrum. Meth.* A **248**, 267–281.

Fauerbach, M. 1992 Diplomarbeit, T. H. Darmstadt.

Gaimard, J.-J. & Schmidt, K.-H. 1991 *Nucl. Phys.* A **531**, 709–745.

Gavron, A. 1980 *Phys. Rev.* C **21**, 230–236.

Geissel, H. 1997 *Nucl. Phys.* A **616**, 316c–328c.

Geissel, H., Schwab, Th., Armbruster, P., Dufour, J. P., Hanelt, E., Schmidt, K. H., Sherrill, B. & Münzenberg, G. 1989 *Nucl. Instrum. Meth.* A **282**, 247–260.

Geissel, H. (and 20 others) 1992*a* *Nucl. Instrum. Meth.* B **70**, 286–297.

Geissel, H. (and 17 others) 1992*b* *Phys. Rev. Lett.* **68**, 3412–3415.

Geissel, H., Münzenberg, G. & Riisager, K. 1995 *Ann. Rev. Nucl. Part. Sci.* **45**, 163–203.

Goldhaber, A. S. 1974 *Phys. Lett.* B **53**, 306–309.

Goldhaber, A. S. & Heckmann, H. H. 1978 *A. Rev. Nucl. Part. Sci.* **28**, 161–205.

Gorshkov, V. A. (and 28 others) 1993 In *Proc. 3rd Int. Conf. on Radioactive Nuclear Beams* (ed. D. J. Morrissey), pp. 81–85. Gif-sur-Yvette: Editions Frontières.

Gosset, J., Gutbrod, H. H., Meyer, W. G., Poskanzer, A. M., Sandoval, A., Stock, R. & Westfall, G. D. 1977 *Phys. Rev.* C **16**, 629–657.

Haight, R. C., Mathews, G. J., White, R. M., Avilés, L. A. & Woodward, S. E. 1983 *Nucl. Instrum. Meth.* **212**, 245–247.

Hill, J. C., Wohn, F. K., Winger, J. A., Khayat, M., Leininger, K. & Smith, A. R. 1988 *Phys. Rev.* C **38**, 1722–1729.

Hüfner, J. 1985 *Phys. Rep.* **125**, 129–185.

Irnich, H. (and 23 others) 1995 *Phys. Rev. Lett.* **75**, 4182–4185.

Joubert, A., Baron, E., Grunberg, C., Larson, J. D., Mittig, W. & Ripoteau, F. 1991 GANIL Report A-91-01.

Kelley, J. H., Austin, S. M., Kryger, R. A., Morrissey, D. J., Orr, N. A., Sherrill, B. M., Thoennessen, M., Winfield, J. S., Winger, J. A. & Young, B. M. 1995 *Phys. Rev. Lett.* **74**, 30–33.

Kolata, J. J., Morsad, A., Kong, X. J., Warner, R. E., Becchetti, F. D., Liu, W. Z., Roberts, D. A. & Jänecke, J. W. 1989 *Nucl. Instrum. Meth.* B **40/41**, 503–506.

Kubo, T., Ishihara, M., Inabe, N., Nakamura, T., Okuno, H., Yoshida, K., Simoura, S., Asahi, K., Kumagai, H. & Tanihata, I. 1990 In *Proc. 1st Int. Conf. on Radioactive Nuclear Beams, Berkeley* (ed. W. D. Myers, J. M. Nitschke & E. Norman), pp. 563–572. Singapore: World Scientific.

Matsuta, K. (and 12 others) 1992 *Nucl. Instrum. Meth.* B **70**, 304–308.

Mercer, M. T., Hill, J. C., Wohn, F. K., McCullough, C. M., Nieland, M. E., Winger, J. A., Howard, C. B., Renwick, S., Matheis, D. K. & Smith, A. R. 1986 *Phys. Rev.* C **33**, 1655–1667.

Morrissey, D. J. 1989 *Phys. Rev.* C **39**, 460–470.

Morrissey, D. J. 1997 In *Proc. 13th Int. Conf. on Electromagnetic Separators and Techniques Related to their Applications, Bad Dürkheim, Germany, 23–27 September 1996* (ed. G. Münzenberg). *Nucl. Instrum. Meth.* B **126**, 316–319.

Morrissey, D. J., Marsh, W. R., Otto, R. J., Loveland, W. & Seaborg, G. T. 1978 *Phys. Rev.* C **18**, 1267–1274.

Morrissey, D. J., Oliveira, L. F., Rasmussen, J. O., Seaborg, G. T., Yariv, Y. & Freaenkel, Z. 1979 *Phys. Rev. Lett.* **43**, 1139–1142.

Mueller, A. C. & Anne, R. 1991 *Nucl. Instrum. Meth.* B **56/57**, 559–563.

Münzenberg, G. 1992 *Nucl. Instrum. Meth.* B **70**, 265–275.

Nolen, J. A. & Harwood, L. 1985 In *Instrumentation for heavy ion nuclear research* (ed. D. Shapira), p. 171. New York: Harwood.

O'Donnell, T. W. (and 10 others) 1994 *Nucl. Instrum. Meth.* A **353**, 215–216.

Okuno, H. (and 22 others) 1994 *Phys. Lett.* B **335**, 29–34.

Orr, N. A. (and 17 others) 1991 *Phys. Lett.* B **258**, 29–34.

Orr, N. A. (and 11 others) 1992 *Phys. Rev. Lett.* **69**, 2050–2053.

Pfaff, R. (and 11 others) 1995 *Phys. Rev.* C **51**, 1348–1355.

Pfaff, R., Morrissey, D. J., Fauerbach, M., Hellström, M., Powell, C. F., Steiner, M. & Winger, J. A. 1996 *Phys. Rev.* C **53**, 1753–1758.

Rehm, K. E. (and 11 others) 1996 *Nucl. Instrum. Meth.* A **370**, 438–444.

Rudstam, G. 1966 *Z. Naturforsch.* **21a**, 1027.

Schmidt, K.-H., Hanelt, E., Geissel., H., Münzenberg, G. & Dufour, J. P. 1987 *Nucl. Instrum. Meth.* A **260**, 287–303.

Schwab, T. 1992 PhD thesis, Universität Geissen.

Sherrill, B. M. 1992 In *Proc. Int. Conf. on Radioactive Nuclear Beams, Louvain la Neuve* (ed. Th. Delbar), pp. 1–20. London: Adam Hilger.

Sherrill, B. M., Morrissey, D. J., Nolen, J. A., Orr, N. & Winger, J. A. 1992 *Nucl. Instrum. Meth.* B **70**, 298–303.

Shimoda, T., Miyatake, H. & Morinobu, S. 1992 *Nucl. Instrum. Meth.* B **70**, 320–330.

Souliotis, G., Morrissey, D. J., Orr, N. A., Sherrill, B. M. & Winger, J. A. 1992 *Phys. Rev.* C **46**, 1383–1392.

Souliotis, G., Loveland, W., Zyromski, K. E., Wozniak, G. J., Morrissey, D. J., Liljenzin, J. O. & Aleklett, K. 1997 *Phys. Rev.* C **55**, R2146–R2149.

Steiner, M. (and 20 others) 1996 *Phys. Rev. Lett.* **76**, 26–29.

Sümmerer, K. & Morrissey, D. J. 1990 In *Proc. 1st Int. Conf. on Radioactive Nuclear Beams, Berkeley* (ed. W. D. Myers, J. M. Nitschke & E. Norman), pp. 122–131. Singapore: World Scientific.

Sümmerer, K., Brüchle, W., Morrissey, D. J., Schädel, M., Szweryn, B. & Weifan, Y. 1990 *Phys. Rev.* C **42**, 2546–2561.

Tanihata, I. 1997 *Nucl. Phys.* A **616**, 56c–68c.

Tanihata, I., Hamagaki, H., Hashimoto, O., Shida, Y., Yoshikawa, N., Sugimoto, K., Yamakawa, O., Kobayashi, T. & Takahasi, N. 1985 *Phys. Rev. Lett.* **55**, 2676–2679.
Tribble, R. E., Burch, R. H. & Gagliardi, C. A. 1989 *Nucl. Instrum. Meth.* A **285**, 441–446.
Van Bibber, K. (and 10 others) 1979 *Phys. Rev. Lett.* **43**, 840–844.
Viyogi, Y. P. (and 14 others) 1979 *Phys. Rev. Lett.* **42**, 33–36.
Webber, W. R., Kish, J. C. & Schrier, D. A. 1990 *Phys. Rev.* C **41**, 547–565.
Winger, J. A., Sherrill, B. M. & Morrissey, D. J. 1992 *Nucl. Instrum. Meth.* B **70**, 380–392.
Wollnik, H. 1987 *Optics of charged particles*. Boston: Academic Press.
Wollnik, H. (and 28 others) 1997 *Nucl. Phys.* A **616**, 346c–351c.
Yamagata, T. (and 11 others) 1989 *Phys. Rev.* C **39**, 873–876.
Yariv, Y. & Fraenkel, Z. 1979 *Phys. Rev.* C **20**, 2227–2243.
Yariv, Y. & Fraenkel, Z. 1981 *Phys. Rev.* C **24**, 488–494.

PHILOSOPHICAL TRANSACTIONS OF THE ROYAL SOCIETY A MATHEMATICAL, PHYSICAL & ENGINEERING SCIENCES